An Automatic Identification System of Agricultural Pests Based on Machine Vision

Zhang Faquan[1,2], Wang Guofu[1,2], Ye Jincai[1], Liu Qinghua[1]

1. School of Information and Communication, Guilin University of Electronic Technology, Guilin 541004, China
2. Key Laboratory Cognitive Radio and Information Processing of the Ministry of Education, Guilin 541004, China

Abstract: An automatic identification system of agricultural pests based on machine vision, image processing and pattern identification was presented. First the hardware system was completed and pests' image which posture helped processing and identifying was obtained. Second image preprocessing was made and total 12 features including color, area, perimeter, fractal dimension and ridgelet edge moment were extracted. Third feature selection was implemented to select 7 features. Finally BP neural network classifier was designed to classify and identify pests. For usual 8 species of pests recognition rate was up to 85.7%. Results show that the system is automatic and high recognition rate and meet the demand of real application.

Keywords: Machine Vision, Image Processing, Automatic Identification, Agricultural Pests

0. Introduction

China is a great agricultural country so that detection and prediction of agricultural pests has become main tasks for all levels plant protection departments. One of the premises of monitoring and controlling pests is classifying accurately pests. At present forecasting method of trapping pests using the black light lamp and counting pests by artificial cognition was adopted widely. It was of poor accuracy and low efficiency in recognition rate. Therefore, accuracy and timeliness of detection and prediction were decreased immensely. This was harm to prevention and control for the agricultural pests. On the other hand, the results of detection and predication were inaccurate and bad timeliness so that pesticides were used heavily and ecologic environment and crops were severely polluted[1-2].

For defects of artificial classification methods, in recent years some researchers presented various automatic classifying pests methods from different aspects through acquiring and analyzing pests' sound and images by using some technological achievements in areas of image processing and pattern identification[3-6]. By making use of feature parameters such as colors, shapes and so on retrieved from pest images, a kind of remote automatic identification system of pests was proposed[7-8]. In order to improve accuracy of classification, matter-elements extension sets algorithm was utilized in pest classification of stored grain pests[9]. Some researchers presented stored grain classification method based on artificial immune algorithm, support vector machine and simulated annealing algorithm[10-11]. Compared with fuzzy partition, nearest neighbor classification method and neural network classification method, it could effectively enhance classification accuracy of stored grain pests[12].

The above pest classification methods showed good classified effect in various applications. However, there were many reasons, such as a large variety of pests, many factors to impact classification results and higher classification accuracy required in real application, so that there were some shortcomings in these pest classification methods[13-14]. Therefore, we proposed

image identification technique based on machine vision and ridgelet analysis to automatically detect and predicate agricultural pests.

1. Detection system

Detection system was shown in Figure 1. The black light lamp was placed on the box with a sink. Pests were lured by light emitted by the black light lamp and fell into the sink through the pipe. Pests' posture was adjusted by running water. When pests past over the visual area of the CCD camera, the latter acquired image sequences of pests in real-time. Image sequences were rapidly sent to image processing system through PCI bus. We classified pests' species and density using ridgelet analysis, image processing, image analysis and pattern identification, and provided decision-making basis for integrated pest control.

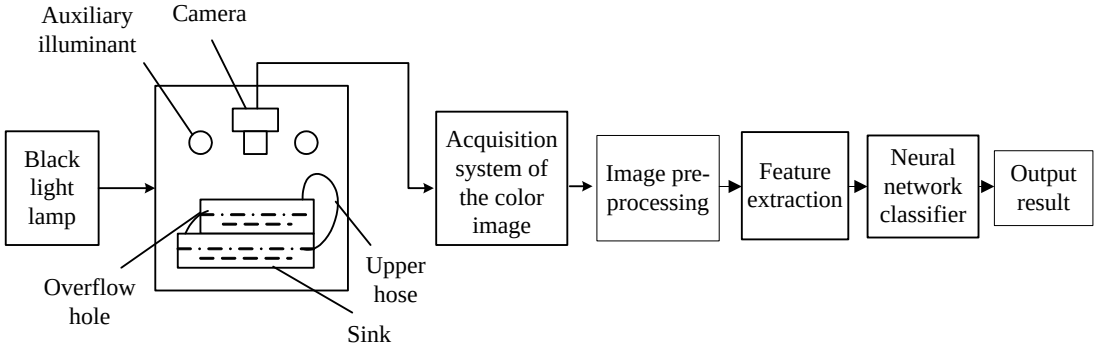

Fig. 1 Flow diagram of detection system

2. Soft development

Soft of the system was developed by Microsoft Visual C++2005. Windows XP was adopted as operating system platform. Overall diagram was shown in Figure 2.

Specific procedure was explained as following:

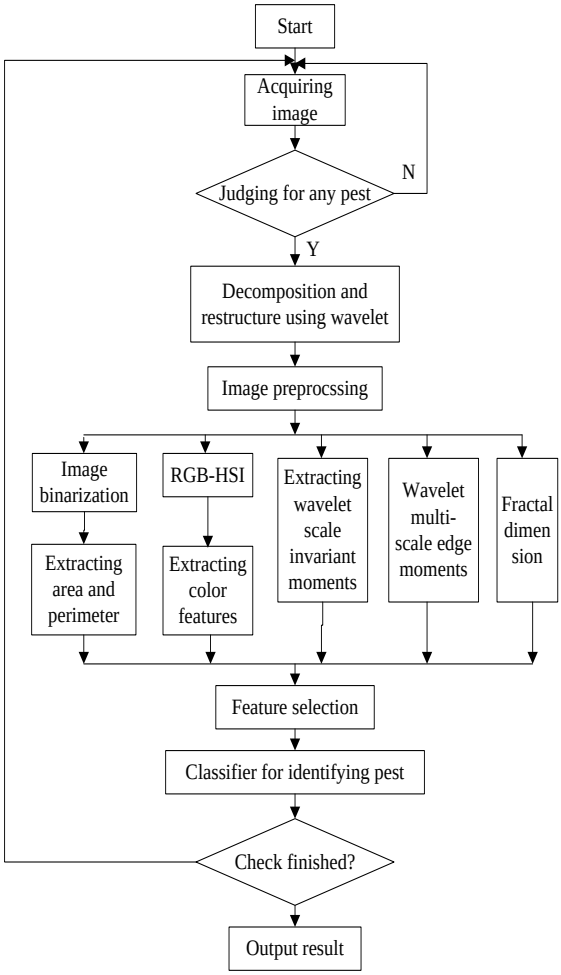

Fig. 2 General flowchart of software system

1) After original image of a pest was acquired, we extracted area feature to judge whether a pest was existed or not in the image. If there were some pests we need process image.

2) Image decomposition using ridgelet transform.

3) Image with noise acquired by a real system was inevitable, so image must be preprocessed in transform domain.

4) Feature extraction. We extracted respectively area, perimeter, color feature, ridgelet scale invariant moment, image's edge moment and fractal dimension.

5) Feature selection. We selected total 12 features, including area, perimeter, six color features, two image edge moments and two fractal dimensions. We impressed six color features into one feature and formed 7 effective features.

6) Classification. We input all features into neural network classifier to identify and classify. Hence, statistical result was output.

3. Feature extraction

3.1 Area and perimeter

3.1.1 Color image gradation processing

Most agricultural pests lured by the black light lamp belonged to moths with various colors and markings. Therefore, we acquired pests' color image by means of the color CCD camera. Area and perimeter of the pests' image were geometric features which described geometric properties of the target area. Before extracting geometric properties, images must be grayed and two-valued. This job was implemented in the copy of the original image.

We grayed the color image using the weighted mean method. We gave different weight to R, G, and B according to importance and other parameters and made weighted mean calculation. That was

$$R = G = B = W_R R + W_G G + W_B B \quad , \tag{1}$$

where W_R, W_G and W_B were respectively weight of R, G and B. If we gave them different values, we got different gray image by weighted mean method. Our eye was high sensitive to green. Our sensitivity to red was lower and it to blue was lowest. When $W_R > W_G > W_B$ was satisfied, we obtained the reasonable gray image. Experimental result showed when $W_R = 0.30$, $W_G = 0.59$, $W_B = 0.11$, or

$$V_{gray} = 0.30R + 0.59G + 0.11B \quad , \tag{2}$$

$$R = G = B = V_{gray} \quad , \tag{3}$$

the image obtained was reasonable.

3.1.2 Image binarization

After image gradation processing, we binarized the image into two-valued image. There were many threshold selection methods. According to real situation of the system, we selected the threshold as following.

1) We extracted gray value of the pixels in the four corner of the image.

2) We sorted four gray values and removed the maximum and the minimum. The average of two middle gray values was acted as gray value of the background. We modified the average and made it the threshold of binarization.

Figure 3 and Figure 4 were Parasa consocia's gray image and binary image respectively.

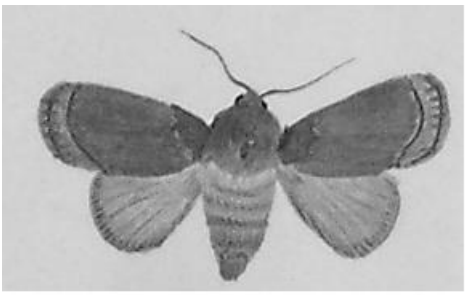

Fig. 3 Parasa consocia's gray image

Fig. 4 Parasa consocia's binary image

3.1.3 Extracting area and perimeter

Given the size of the image $f(x, y)$ was $M \times N$.

(1) Area was defined as

$$A = \sum_{x=1}^{M} \sum_{y=1}^{N} f(x, y) \quad . \tag{4}$$

Area A of the object was total number of pixels involved the object in the image.

(2) Perimeter was defined as

$$P = A - SUM(in) \quad , \tag{5}$$

where A was the area of the object and $SUM(in)$ was total number of pixels which 4-neighborhood were pixels of the object.

According to the above two equations, we extracted area and perimeter of the object. Processing result to Parasa consocia was shown in Figure 5.

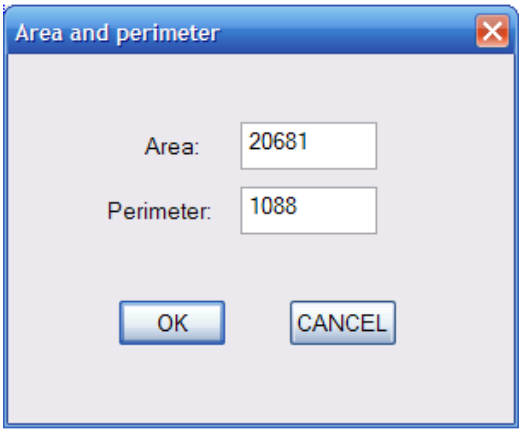

Fig. 5 Interface of area and perimeter's feature extraction

3.2 Color feature of the object

Color image was expressed by component of R, G and B. Three components of R, G and B had a higher correlation. If we determined one color we must consider its three components. This increased difficulty of analysis. In order to reduce correlation of various features in color feature space and to implement conveniently color image segmentation, we always changed RGB image into other color feature space in practice.

Visual sense to color near human vision was hue, saturation, intensity space, shorten HSI space. HSI model had two bases. First I component had nothing to color information. Second H and S components connected with style which man felt color. HSI space was intuitive and fit for human visual property. Hence HSI model was very fit for color image processing based on human visual system. Transformation from RGB to HSI was

$$H = \cos^{-1}\left\{\frac{(R-G)+(R-B)}{2\sqrt{(R-G)^2+(R-B)(G-B)}}\right\} \qquad R \neq G \quad or \quad \mathrm{R} \neq B, \tag{6}$$

$$S = 1 - \frac{3}{R+G+B}[\min(R,G,B)] \ , \tag{7}$$

$$I = \frac{R+G+B}{3}. \tag{8}$$

In the equation (6) H was formed by R, G and B through nonlinear transformation. The effect of H was obsolete when saturation was low. Especially in region where saturation was zero H was meaningless. In other words, when S = 0, H was meaningless. Then we defined H was zero. Meanwhile, when I = 0, S was also meaningless and it was defined as zero.

Since HSI color space was near human visual properties, discrimination of change of HSI for human eye was stronger than discrimination of change of RGB. In addition, every uniform color region in color image in HSI space was corresponding to one relatively uniform hue. It also indicated the hue could segment color region.

Most agricultural pests were colorful and color information became important characteristic to classify pests. Some pests were named by main color, such as Parasa consocia, Amsacta lactinea, Deilephila elpenor, Euhampsonia cristata, and so on.

We extracted seven colors in all, including red, yellow, green, cyan, blue, purple, black. Meanwhile we extracted five morphological features for every color. They were listed as follows.

(1) Area. It was defined as total pixel number A in a specific color.

(2) Perimeter. Total number of pixels P which were at edge to a specific color.

(3) Width. Maximum pixel number in horizontal direction to a specific color.

(4) Height. Maximum pixel number in vertical direction to a specific color.

(5) Roundness. A ratio of area A to perimeter P was written as

$$\gamma = \frac{A}{P}. \tag{9}$$

We gave a new definition of roundness to reduce effect of noise. The higher value indicated the shape of the specific color was rounder. The small value indicated the roundness of the specific color was weaker. Its smallest value was 1 to show that the color was composed by some points or lines.

We only counted seven usual colors related to pest identification. Through extensive observation and experiment we determined range of H value for the every color in Table 1.

Tab. 1 Range of H value for various colors

color	H
red	0—20,340—360
yellow	40—70
green	85—140
cyan	160—200
blue	200—260
purple	280—320

In light of Tab. 1, we extracted color features for Parasa consocia as shown in Figure 6.

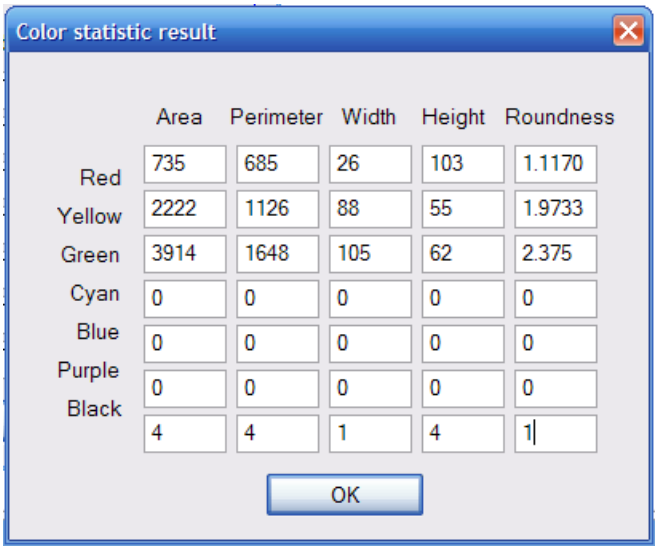

Fig. 6 Feature extraction interface of colors

From result of color count in Tab. 1, Parasa consocia had four colors. They were respectively red, yellow, green and black. Among of them green was main color and its area, perimeter and roundness were all biggest. Black had only four pixels which was two eyes of Parasa consocia.

3.3 ridgelet scale invariant moment

Invariant moment theory was a relatively mature method. There were two problems in moment method. One was that its computation was too huge. The other was that high-order moment was affected mostly by noise. In light of localization thought of Fourier transformation, we hoped make moment method reflecting related information into hierarchical localization. We developed ridgelet moment of two dimension based on ridgelet invariant moment of one dimension[15].

If conjugate filter $H(\omega)$ had $r+1$ order smoothness at zero, we expanded $f(x,y)$ in two-dimension ridgelet formed by $H(\omega)$ and got approximate coefficient $a_{m,n}(j)$. Given $p,q \le r$, two dimension ridgelet moment of $(p+q)$ order based on ridgelet coefficient was written as

$$W_{pq} = 2^{-(p+q+1)j} \sum_{m,n \in z} m^p n^q a_{m,n}(j) \tag{10}$$

where m and n were index of pixel, their range were the size of image M and N, respectively.

3.4 ridgelet image edge moment

Shape was an important characteristic to describe content of the image. Shape usually associated with the object in the image. Therefore, we first extracted image edge to obtain description of the shape characteristic. We extracted multi-scale edge information of the object using ridgelet module maximum method. Then we classified the object based on seven edge's invariant moment features in multi-scale.

For the image which size was $M \times N$, its two order moment of multi-scale edge function $WT(i, j)$ was defined as

$$m_{pq} = \sum_{i=1}^{M} \sum_{j=1}^{N} i^p j^q WT(i, j) \quad . \tag{11}$$

Central moment was defined as

$$\mu_{pq} = \sum_{i=1}^{M} \sum_{j=1}^{N} (i - \bar{i})^p (j - \bar{j})^q WT(i, j) \quad , \tag{12}$$

where

$$\bar{i} = \frac{m_{10}}{m_{00}}, \quad \bar{j} = \frac{m_{01}}{m_{00}}$$

We normalized central moment and defined normalized central moment as

$$\eta_{pq} = \frac{\mu_{pq}}{\mu_{00}^{p+q+1}} \quad . \tag{13}$$

We got seven edge's invariant moments with invariant characteristic of rotation, scale and shift. They were written as

$$\begin{aligned}
I_1 &= \eta_{20} + \eta_{02} \\
I_2 &= (\eta_{20} - \eta_{02})^2 + 4\eta_{11}^{\ 2} \\
I_3 &= (\eta_{30} - 3\eta_{12})^2 + (\eta_{03} + 3\eta_{21})^2 \\
I_4 &= (\eta_{30} + \eta_{12})^2 + (\eta_{03} + \eta_{21})^2 \\
I_5 &= (\eta_{30} - 3\eta_{12})(\eta_{30} + \eta_{21})\left[(\eta_{30} + \eta_{12})^2 - 3(\eta_{21} + \eta_{03})^2\right] + (\eta_{03} - 3\eta_{21})(\eta_{03} + \eta_{21})\left[(\eta_{03} + \eta_{21})^2 - 3(\eta_{12} + \eta_{30})^2\right] \\
I_6 &= (\eta_{20} - \eta_{02})\left[(\eta_{30} + \eta_{12})^2 - (\eta_{03} + \eta_{21})^2\right] + 4\eta_{11}(\eta_{30} + \eta_{12})(\eta_{03} + \eta_{21}) \\
I_7 &= (3\eta_{12} - \eta_{03})(\eta_{30} + \eta_{12})\left[(\eta_{30} + \eta_{12})^2 - 3(\eta_{21} + \eta_{03})^2\right] + (\eta_{30} - 3\eta_{21})(\eta_{03} + \eta_{21})\left[(\eta_{03} + \eta_{21})^2 - 3(\eta_{12} + \eta_{30})^2\right]
\end{aligned} \tag{14}$$

Table 2 was result to Parasa consocia and Agrotis tokionis based on the above theory.

Tab.2 Ridgelet image edge moments of Parasa consocia and Agrotis tokionis

Features	Parasa consocia	Agrotis tokionis
I1	6632.57	11272.2
I2	1.49518e+007	3.70104e+007
I3	1.29436e+010	7.2817e+010
I4	1.0349e+009	4.79475e+010
I5	-4.56532e+018	2.74337e+021
I6	-3.94007e+012	2.32561e+014
I7	-2.17933e+018	6.41466e+021

3.5 Fractal dimension

To develop further fractal phenomenon, we need find some quantitative indexes to describe fractal characteristic in order to detect and classify fractal phenomenon. Several indexes had been proposed, such as fractal dimension, Lyapounov index, relevant dimension, kolmogorov entropy, and so on. We extracted fractal dimension to indicate fractal characteristic using ridgelet analysis[16-17].

Given the signal was decomposed using ridgelet at resolution 2^j into $D_{2^j} f$ and its energy was $\sigma_{2^j}^2$, we had the expression

$$\sigma_{2^j}^2 = 2^{2H} \cdot \sigma_{2^{j+1}}^2 . \tag{15}$$

For two dimension image signal, the above expression was given by

$$\sigma_{2^j}^2 = 2^{4H} \cdot \sigma_{2^{j+1}}^2 \quad . \tag{16}$$

Hence, we obtained fractal parameter H through calculating energy ratio of image detail signal in two adjacent scales.

After decomposed using ridgelet, image was divided into 4 parts. Three parts belonged to high frequency. So we composited these three parts into one result using Euclid distance equation. Table 3 showed the result extracted using fractal dimension to Parasa consocia and Agrotis tokionis. Fractal dimension 1 was fractal parameter H based on energy ratio of scale j=2 and j=1. Similarly, Fractal dimension 2 was energy ratio of scale j=3 and j=2.

Tab. 3 Fractal dimensions of Parasa consocia and Agrotis tokionis

Pests name	Fractal dimension 1	Fractal dimension 2
Parasa consocia	0.389737	0.130522
Agrotis tokionis	0.757513	0.244816

After feature selection, we selected finally 12 features as optimal features to classify and identify pests. Figure 7 resulted in feature selection for Parasa consocia.

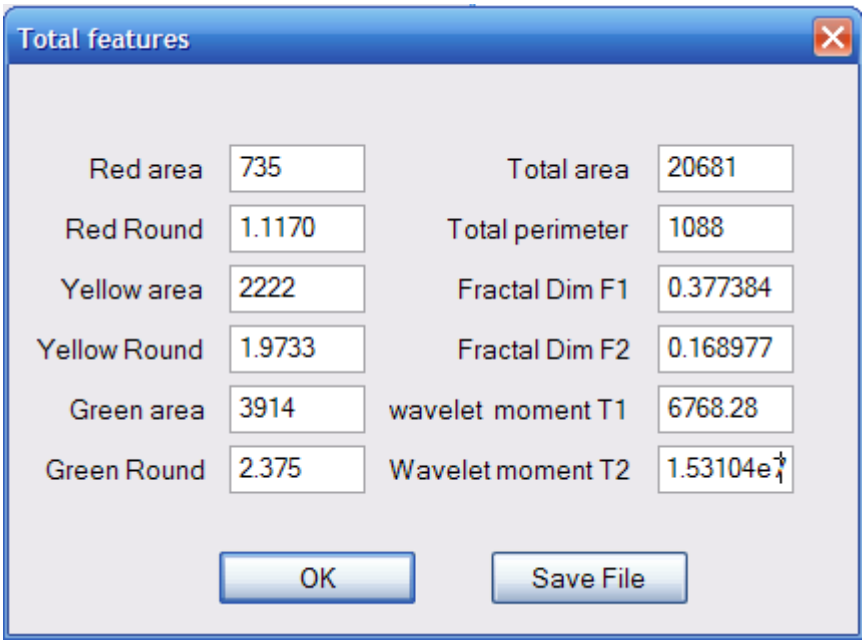

Fig. 7 All features of Parasa consocia

We processed usual pests including Eterusia aedea formosana, Parasa consocial, Marumba sperchius, beet armyworm, maize moth, cotton bollworm, mythimna separate. Recognition rate using BP neural network classifier for these usual pests was up to 85.7%.

4. Conclusions

By using machine vision and image identification techniques, we completed image preprocessing, feature extraction and feature selection and determined 12 features to identify pests. These features included color, area, perimeter, fractal dimension and ridgelet edge moments. Finally we classified pests using BP neural network classification. They were respectively Eterusia aedea formosana, Parasa consocial, Marumba sperchius, beet armyworm, maize moth, cotton bollworm, mythimna separate. Recognition rate was up to 85.7%.

There were more than 30 spices of pest in china. To better meet detection demand of agricultural pests, we need further research the method to identify more pests. Only one classification was hard to meet demand of identification accuracy. Then we should extract more texture and edge features and combine with other pests' factors including location, season, crops destroyed and similarity of pests. Therefore, we separated identification of pests into several small sub-module identification problems and jointed data fusion to further improve speed and accuracy of identification.

Acknowledgements

The authors wish to thank the helpful comments and suggestions from my teachers and colleagues in Guangxi Key Lab of Wireless Wideband Communication & Signal Processing at Guilin. This work was supported in part by NSFC under Grant No. 61362020 and No.61102115, Guangxi Natural Science Foundation under Grant No.2013GXNSFAA019327 and 2012GXNSFBA053177, Guangxi Key Lab of Wireless Wideband Communication & Signal Processing under Grant No. 20130112.

References:

[1] Jatav, K. S. and J. Dhar, Hybrid approach for pest control with impulsive releasing of natural enemies and chemical pesticides: A plant-pest-natural enemy model. Nonlinear Analysis-Hybrid Systems, 2014, 12: p. 79-92.

[2] Peng, Yingqiong, Yinglong Wang, Jianjun Tang, et al. Study on rice pest insect and disease diagnosis expert system in Jiangxi Province using BP neural network. Proceedings - 2010 3rd IEEE International Conference on Computer Science and Information Technology, ICCSIT 2010. Chengdu, China. IEEE Computer Society. 2010. p.432-434.

[3] Han, Antai, Xiaohua Guo, Zhong Liao, et al., Classification of agricultural pests based on compressed sensing theory. Nongye Gongcheng Xuebao/Transactions of the Chinese Society of Agricultural Engineering, 2011, 27(6): p. 203-207.

[4] Sundstrom, J. F., A. Albihn, et al., Future threats to agricultural food production posed by environmental degradation, climate change, and animal and plant diseases - a risk analysis in three economic and climate settings. Food Security, 2014, 6(2): p.201-215.

[5] Marcos, W. P., M. V. M. Ferreira, A. P. Cortes, et al. Markovian decision problems applied in pest control of agriculture production systems. IFAC Proceedings Volumes (IFAC-PapersOnline). Fortaleza, Ceara, Brazil. IFAC Secretariat. 2013. p.159-164.

[6] Mei, L., Z. G. Guan, H. J. Zhou, et al. Agricultural pest monitoring using fluorescence lidar techniques Feasibility study. Applied Physics B: Lasers and Optics. Tiergartenstrasse 17, Heidelberg, D-69121, Germany. Springer Verlag. 2012. p.733-740.

[7] Elek, Naomi, Roy Hoffman, Uri Raviv, et al., Novaluron nanoparticles: Formation and potential use in controlling agricultural insect pests. Colloids and Surfaces A: Physicochemical and Engineering Aspects, 2010, 372(1-3): p. 66-72.

[8] Del Aguila, Isabel Maria, Jose Del Sagrado, Samuel Tunez, et al. Seamless software development for systems based on Bayesian networks: An agricultural pest control system example. ICSOFT 2010 - Proceedings of the 5th International Conference on Software and Data Technologies. Athens, Greece. Inst. for Syst. and Technol. of Inf. Control and Commun. 2010. p.456-461.

[9] Yang, Minli, Xiaomei Ma, and Fengxia Hao. Insecticidal activity of extract from Cynanchi Auriculati against agricultural pests. Advances in Intelligent and Soft Computing. Sanya, China. Springer Verlag. 2012. p.419-424.

[10] Zhang, Jianhua, Ronghua Ji, Xue Yuan, et al., Recognition of pest damage for cotton leaf based on RBF-SVM algorithm. Nongye Jixie Xuebao/Transactions of the Chinese Society of Agricultural Machinery, 2011, 42(8): p. 178-183.

[11] Zou, Xiuguo and Weimin Ding, Design of processing system for agricultural pests with digital signal processor. Journal of Information and Computational Science, 2012, 9(15): p. 4575-4582.

[12] Lzzo, V. M., D. J. Hawthorne, et al., Geographic variation in winter hardiness of a common agricultural pest, Leptinotarsa decemlineata, the Colorado potato beetle. Evolutionary Ecology, 2014, 28(3): p.505-520.

[13] Xie, Chunyan, Dake Wu, Chaoyong Wang, et al., Insect pest leaf detection system based on information fusion of image and spectrum. Nongye Jixie Xuebao/Transactions of the Chinese Society for Agricultural Machinery, 2013, 44(SUPPL.1): p. 269-272.

[14] Kan, I., Y. Motro, et al., Agricultural Rodent Control Using Barn Owls: Is It Profitable?. American Journal of Agricultural Economics, 2014, 96(3): p.733-752.

[15] Ravisankar, H., U. Sreedhar, et al., Expert system for insect pests of agricultural crops. Indian Journal of Agricultural Sciences, 2014, 84(5): p.607-611.

[16] Jiuxi, Li, Wang Chunshan, Li Qiang, et al., The design of the SMS platform for chinese jujube diseases and insect pest diagnosis. Journal of Convergence Information Technology, 2012, 7(23): p. 25-33.

[17] Taki, H., K. Tabuchi, et al., Spatial and temporal influences of conifer planted forests on the orchard pest Plautia stali (Hemiptera: Pentatomidae). Applied Entomology and Zoology, 2014, 49(2): p.241-247.